B1.   Progress made against the Approved Objectives, Targets & Timelines

Nanoparticle based approach to enhance the AMP efficacy against AMP resistant bacteria

Dr Anupam Nath Jha

Assistant Professor

Molecular Biology and Biotechnology

Tezpur University,

Nappam, Assam (784028)

Contact - 03712-275416, 8876236119

E-mail - anjha@tezu.ernet.in

Dr. Suman Jha

Assistant Professor,

Department of Life Science,

National Institute of Technology Rourkela,

Odisha 769008

Contact: 0661-2462687, 7381108201

E-mail: jhas@nitrkl.ac.in

Approved objectives, Targets and timelines

Tezpur University:

Period of study (in months)	Achievable targets
6	Identification and data collection of antimicrobial peptides (AMP)
12	Computational analysis of different structural characteristics and functional properties of AMP
18	Interaction study of NP-AMP using molecular docking
24	Time based evaluation of interaction mechanism of NP-AMP interface by molecular dynamics simulation
30	Study of the importance of functional groups on NP surface affecting the interaction pattern
36	Formulation for enhancing the efficacy of AMP

NIT, Rourkela:

Period of study	Achievable targets
6 Months	Synthesis and characterization of photocatalytic nanoparticles like ZnONP, IONP, AgNP, Alum nanoparticle etc.
12 Months	Binding thermodynamics of identified AMPs with the synthesised nanoparticles, extensively, using ITC. Conformational dynamics of AMPs upon conjugation or binding to the nanoparticle using CD spectropolarimeter, ATR-FTIR, etc.
18 Months	Modification of accessible functional groups of the nanoparticles (according to the simulation results), and characterization of the modifications
24 Months	Investigation of binding thermodynamics and conformational dynamics of AMPs upon conjugation with the surface modified nanoparticles
30 Months	Investigation of the AMP-NP conjugates antimicrobial activity against sensitive and membrane based resistant bacteria
36 Months	Comparative study of the AMP-NP conjugates antimicrobial activity against enzyme based, membrane base resistant bacteria with sensitive bacteria

Consolidated progress report

1. **Equipment purchasing & Manpower recruitment**

   Two GPU-based computer workstations (NVIDIA Tesla K40 GPU card in Dell Poweredge R730) have been purchased and installed successfully.

   a. One JRF (Sapna Mayuri Borah) had been recruited (November 1st, 2016 to October 31st, 2017)
   b. One JRF (Zaved Hazarika) had been recruited (November 1st, 2017 to April 30th, 2018).
   c. One JRF (Sapna Mayuri Borah) had been recruited (May 1st 2018 to December 31st 2018)
   d. One SRF (Zaved Hazarika) had been recruited (January 1st 2019 to April 17th 2020)

2. **Visit to collaborating institution**

   i) Dr. Anupam Nath Jha (PI, Tezpur Unuiversity, Host Institute) visited National Institute of Technology Rourkela (2nd – 8th July 2017) to discuss the progress on collaborative work.

   ii) Dr. S Jha (PI, Partner Institute) has visited Tezpur University (29th – 31st October, 2018) to discuss the collaborative work.

3. **Attending conferences**

i) Dr A N Jha (PI) has attended an **International Conference** on the Interface of Physical, Chemical and Biological Sciences at Dr. H. S. Gour Vishwavidyalaya Sagar, Madhya Pradesh during January 11-13, 2017

ii) Ms Sapna Mayuri Borah (JRF) has attended **two conferences**:

 a. National Conference on Chemical Physics, 20th -21st March 2017, at Assam University, Silchar.

 b. Breaking Barriers Through Bioinformatics & Computational Biology, 31st July – 1st August, 2017, at ScFBio, IIT Delhi.

iii) Zaved Hazarika (JRF) has attended Computer Aided Drug Design for Human Pathogens (CADDHP), Tezpur University, Tezpur during 12th – 17th, February, 2018.

iv) Zaved Hazarika (JRF) has attended an "International Conference on Bioinformatics (InCoB-2018)" at JNU, New Delhi

v) Dr. A N Jha (PI) has attended an International Conference on "Systems and Processes in Physics, Chemistry, and Biology" at Assam University, Silchar in Jan 2019

vi) Dr. A N Jha (PI) has attended a GIAN program on "Bio production in Photosynthetic Microbes" at IIT, Kharagpur

4. Research Work

Antimicrobial peptides and proteins (AMP) have served a fundamental role in the successful evolution of complex multicellular organisms. In the world where emergence of resistant bacterial strains against conventional antibiotics is a severe threat to public health worldwide, these AMP have spawned considerable commercial effort to create new classes of anti-infective therapeutics [1]. They carry a fundamental structural shape in which clusters of hydrophobic and cationic amino acids are spatially organized in discrete sectors of the molecule rendering it an `amphipathic' design. The cationic nature of AMP allows them to interact electrostatically with anionic fraction of accessible bacteria surface [2].

The emerging multidrug resistance has also strategized the use of nanoparticles (NPs) in combating the scenario. Many advances have led to the conjugation of AMPs and NPs via non-covalent interactions to enhance antimicrobial activity [3]. The high surface to volume ratio of NP helps higher incorporation of ligands, thereby resulting in multivalency at the NP-peptide/protein interface. Functionalized NP has been an effective way to enhance specificity and efficacy of nanoparticle based delivery systems. They also provide multivalent interactions in the biological system[4]. With the help of accessible functional groups, the interaction and binding with the components of bacterial membrane like lipopolysaccharide (LPS) can be moderated. Binding initiates' receptor mediated endocytosis (RME), thereby paving way to successful delivery of drugs or AMP[5]. We have simulated NP-protein system as part of the project to understand the interactions at the interface. Our choice of nanoparticle is silver nanoparticle (AgNP), which is FDA approved and has reported antimicrobial properties[6]. Nisin and Bovine Lactoferrin (BLF) are the selected anti-microbial peptide and protein components respectively.

With the emerging antibiotic resistance, antimicrobial peptides and proteins (AMP) have significantly helped in the evolution of therapeutic design [7, 8]. These biomolecules are specific in their fundamental structural shape and charge. Hydrophobic and cationic amino acids clusters are

4

spatially ordered in distinct sectors of the molecule rendering it an `amphipathic' nature[9, 10]. Due to the charged nature, electrostatic interactions are facilitated at the anionic bacterial cell surface. These interfacial interactions lead to the disruption of the cellular membrane causing death of the microbe[11, 12]. The mechanism by which the AMP succeeds in doing so is not yet fully known. In order to formulate and enhance the efficacy of the AMP, it is important to understand its mode of action, more precisely the interfacial interaction between AMP and lipid membranes. Experimental techniques have helped in framing a few hypotheses for the mechanism; however, these studies are limited to retrieve a cellular overview only. A clear understanding on the molecular details of the interaction is not yet available. In such a scenario, a fraction of *in silico* techniques have now emerged that can assist experimental data and shed light on the atomistic details of the interactions. Molecular modeling and simulation are state of art techniques that have found immense use to extract molecular level information at several biointerfaces. AMP structures can be simulated with lipid membranes to gain insights into the time averaged molecular motions at the interface of the two systems.

Work done at Tezpur University

1) **Interaction between Nisin and AgNP:**

Nisin is a small (34 amino acids) amphiphilic peptide, produced by specific strains of *Lactococcuslactis*. 13 out of 34 amino acids are post-translationally modified of helps in formation of five (β-methyl) lanthionine rings[13, 14].

The molecular dynamics (MD) simulation of the AgNP core and nisin was performed by GROMACS 5.0.4[15] using the GROMOS96 54A7 force field parameter set. MD simulation study indicated the degree of freedom of C-terminus and hinge region residues, which is supposed to interact with bacterial membrane for lipid-II independent insertion, hence onsets the antimicrobial action. RMSD showed that the complex is stable during the simulation with least fluctuations in the structure of peptide and the core (Fig. 1). Analysis of the individual residues involved in interaction at the interface that the residue numbers 22nd-26th and 31st-34th have come closer to the interface than the N-terminal.
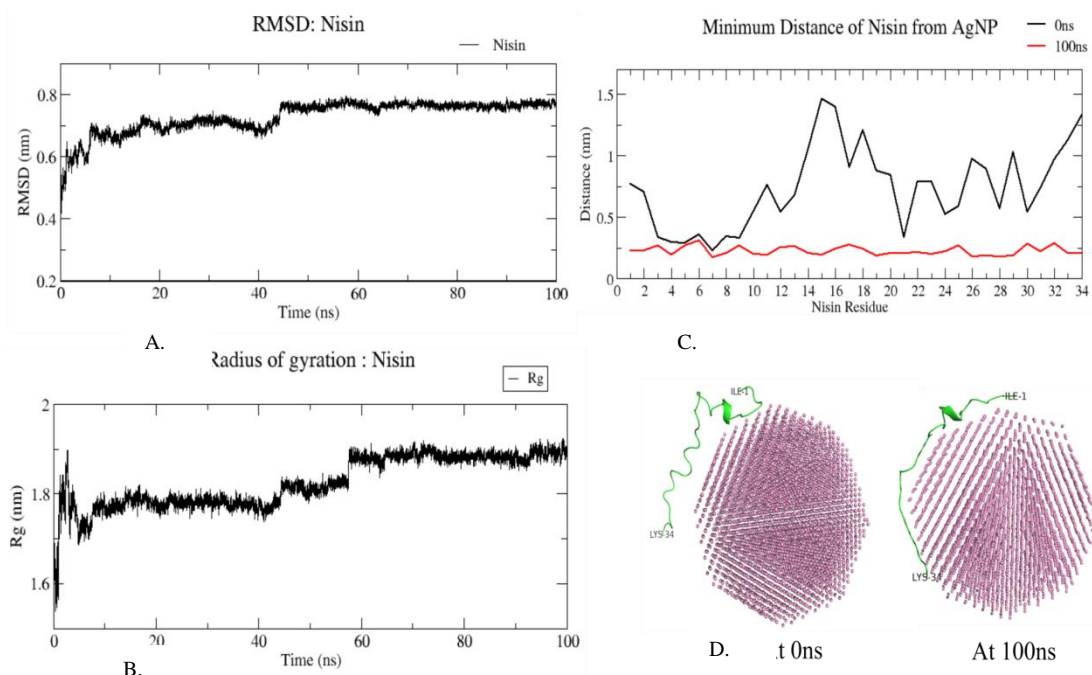
Figure. 1. A- RMSD and B- Rg of Nisin in the Nisin-AgNP complex simulation. C- Distance of Nisin residues from AgNP at 0 and 100ns. D- Nisin-AgNP complex at 0 and 100ns.

2) Interaction between BLF and AgNP:

BLF is a glycoprotein which belongs to the transferrin family of proteins. It is monomeric and multifunctional in nature. BLF has the capability of binding to Fe^{3+} metal and anion (CO_3^-) ligands which is a characteristic function of the transferrins[16]. Structural information is retrieved from the Protein Data Bank (PDB ID: 1BLF) which is X-ray crystallized at a resolution of 2.8Å[17], available for residue length 5 to 676. The protein folds into two lobes (N- and the C-). The lobes are divided into two domain regions, N1, N2 in N- lobe while C1 and C2 in the C-lobe. A hinge region connects the two lobes in the form of a helix[17].
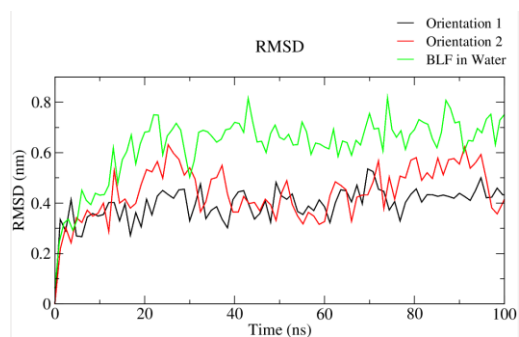
A.
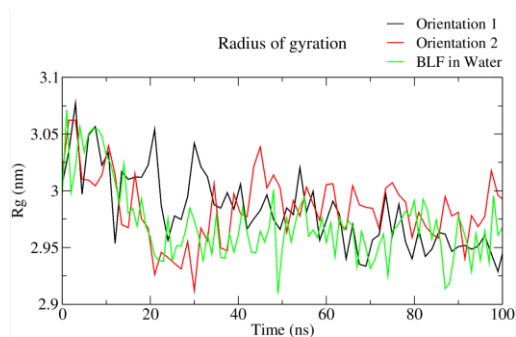
B.
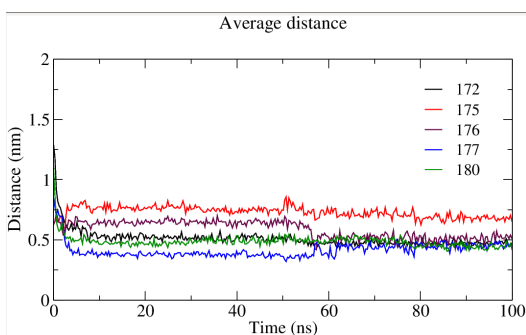
C.
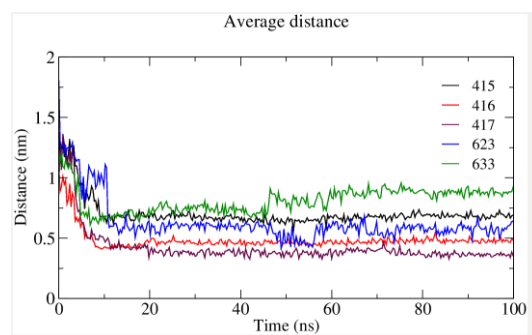
D.
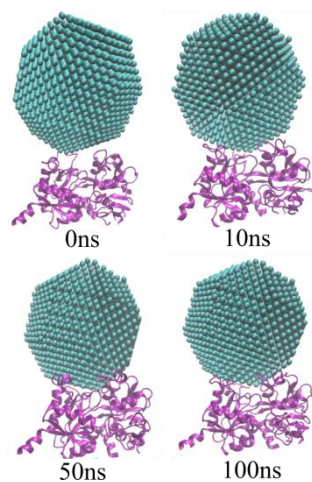
E.
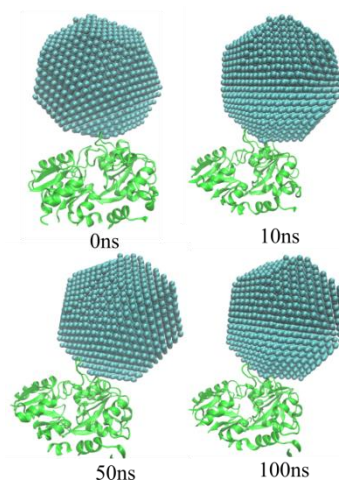
F.

Figure.2. A- RMSD and B- Rg. C- and D- Closest few residues revealed at the NP-Protein interface estimated by Distance Analysis at the N- and C-lobe respectively. E- and F- Snapshots at 0, 10, 50 and 100ns of simulation for the NP placed near the N- and C-lobe respectively.

Molecular dynamics simulation results have been performed in Gromacs 5.1.4 and the trajectories have been analyzed. RMSD deviations tend to be lower in the conjugate systems as compared to the protein simulations indicative of the fact that in the presence of NP, the system seems to be stabilized over the period of time (Fig.2-A). The Rg (Fig.2-B) seems to fluctuate more for the conjugates, due to more movement observed in the lobes of BLF. Distance analysis (Fig.2-C,D) helps reveal a set of 5 residues at both the lobes that are seen to be at the closest distance in the NP-protein interface. The nanoparticle tends to moves towards the active site. Such a behavior may be accounted to the probable interactions at the interface (Fig. 2-E,F).

3) Interaction between Dermicidin and Lipid Membrane

An anionic human AMP, dermicidin was recently discovered for which the mechanism of action is not fully known[18]. Dermicidin (DCD) is a 47 amino acid long anionic peptide which is a valuable means for innate host defense. This AMP is largely secreted by epithelial cells, and also present in neutrophil granules and other cell types [18, 19]. Like other peptides, the mechanism of dermicidin action is not clearly known. In order to elucidate the interaction mechanism, we have performed simulation studies of dermicidin with known model bacterial lipid membranes (POPG). The initial NMR structure for dermicidin is retrieved from RCSB PDB[20] against the PDB ID, 2NDK[21]. POPG (2-oleoyl-1-pamlitoyl-sn-glyecro-3-glycerol), a negatively charged molecule, is an ideal choice of lipids to mimic bacterial membranes[22]. The initial coordinates for 256 lipids are built using MEMGEN builder[23]. Following this we have performed molecular dynamics simulation in Gromacs v5.1.4[24]. All the systems are minimized, equilibrated in both NVT and NPT conditions for 1ns and 5ns respectively. Subsequently, the lipid and AMP are individually simulated for 100 and 200ns respectively to consider the independent motions in the systems. A simulation run for 100ns is performed for the complex of POPG and AMP for 100ns.

Analysis:

Simulation results have shown distinct differences in the peptide conformation in the presence and absence of lipids. The peptide initially shows marked conformation changes in the 200ns simulation in water alone (Fig.1-a), while the same is not observed for the peptide when in complex with the lipid (Fig. 1-b). The backbone differences are determined by the Root mean square deviation (RMSD), shown in Fig. 2. As is evident, the RMSD for the peptide is higher than the counterpart. Principal component analysis is performed to understand the conformational space of the peptide

8

both in the control and peptide in complex (Fig. 3). In order to understand the interface of the POPG and dermicidin peptide, we calculated the number of contacts between the two components at a cut-off distance of 7nm, as depicted in Fig. 4. The structural changes are recorded in the lipid surface as bends that occur at the lipid surface.
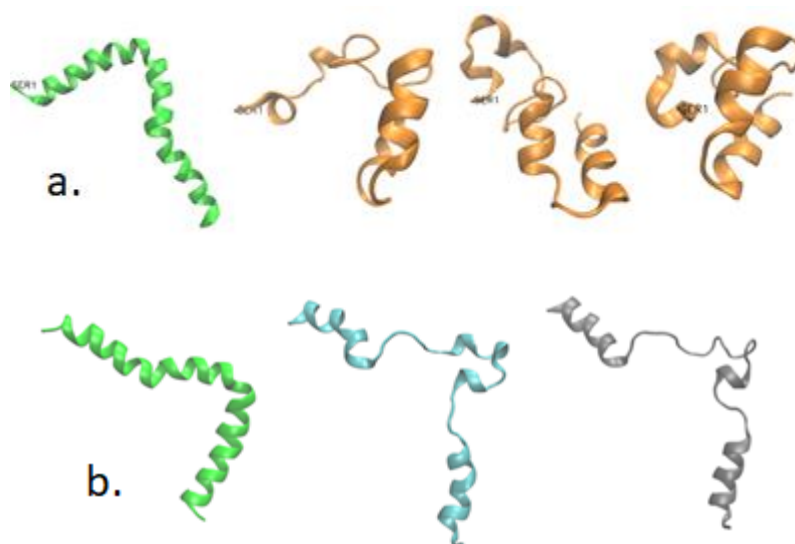
Figure 3. Snapshots at a- 0, 50, 100 and 200ns for dermicidin in water. The initial conformation is shown by a green colour. b- 0, 50 and 100ns for dermicidin in complex with POPG
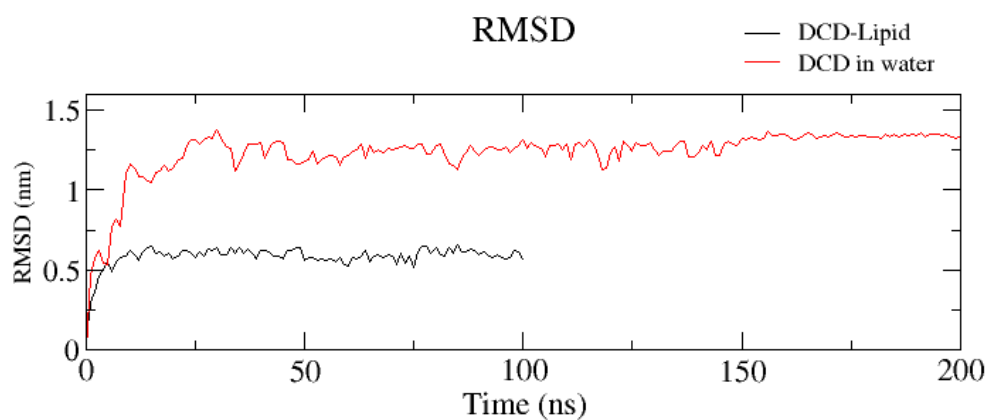
Figure 4. RMSD of DCD in water and with POPG (lipid)
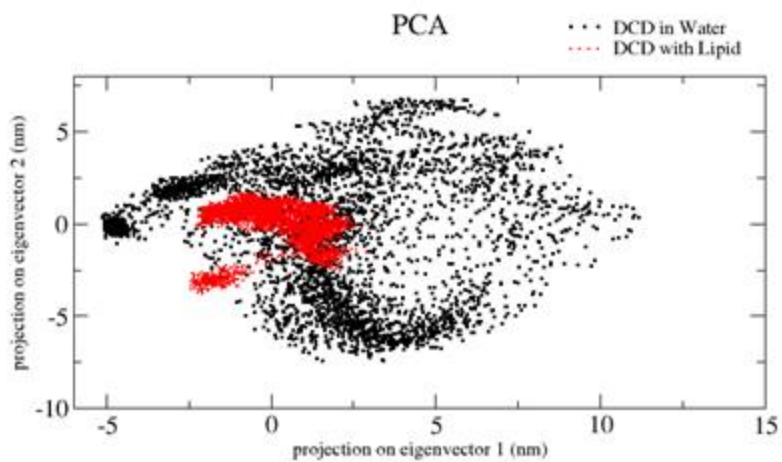
Figure 5. Principal component analysis
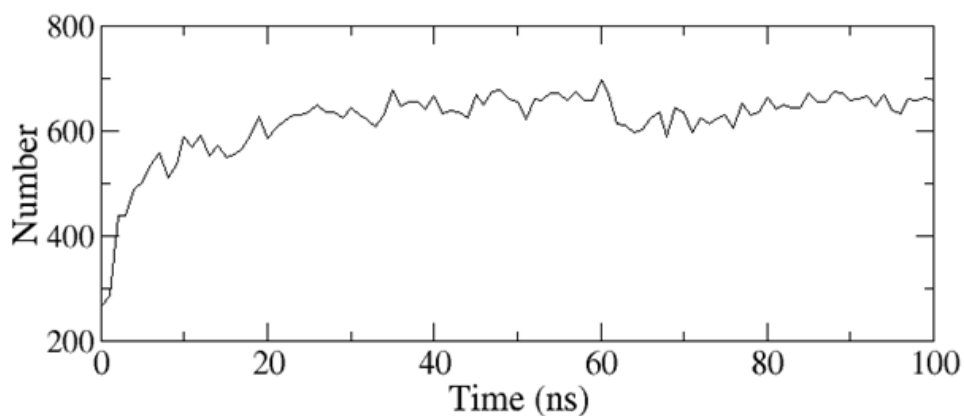
Figure 6. Number of contacts between DCD and lipids as a function of time.
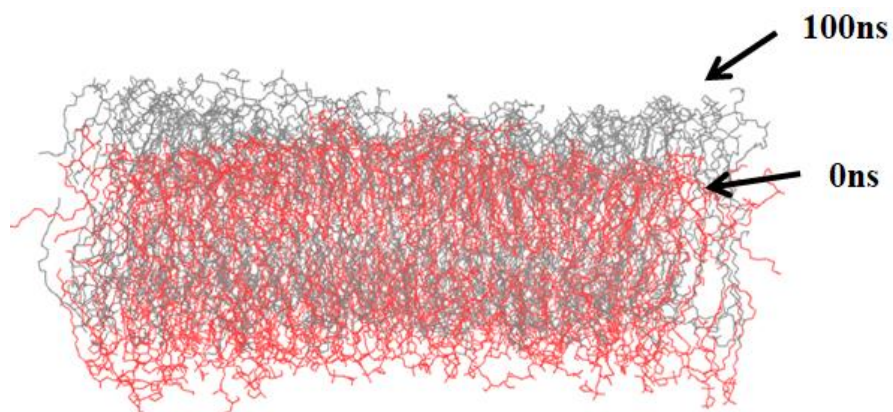
Figure 7. Structural changes in the lipid surface

Work done at NIT Rourkela

1. Characterization of AgNP

The time dependent synthesis of AgNP was initially visualized through the color change, from a colorless to dark brown solution. Further, the synthesis was confirmed by a characteristic SPR peak at 392 nm. Later, the AgNP were subjected to sephadex G-100 for SEC to separate differently sized AgNP monitored through SPR peak using UV-visible spectrometry[25] (Figure 6). Figure 6a shows the AgNP-specific SPR peak of all the eluants collected from SEC at different retention times. The SPR peak of AgNP was found to be 388 nm, which is attributed to the intrinsic energy band-gap exhibited because of electronic transition from valence band to the conduction band upon adsorption of 388 nm photon. All the fractions collected through SEC have single SPR (Figure 6a), confirming the size homogeneity of AgNP[25]. Figure 6b shows the XRD pattern of powder AgNP obtained by evaporation of colloidal suspension of AgNP at 37 °C. The diffraction peaks at 44.6°, 51.9° and 76.6° 2θ angles are indexed to the plane of (111), (200) and (222) indices, respectively. The assigned plane of the diffraction pattern of AgNP corresponds to face-centered cubic crystallization, as per the JCPDS reference code of 01-1164. The average size of AgNP can be calculated using Debye's Scherrer's equation $(K*\lambda/\beta*\cos\theta)$, where λ is the wavelength of X-ray $(1.540 \times 10^{-10}$ m), K= 0.9, proportionality coefficient (shape factor), θ is the Bragg's angle, and β is the full width at half maximum in radians. Hence, the average size of AgNP calculated using Scherrer's equation is 18 ±3 nm. To obtain a better resolution and surface morphology of nanoparticles after purification, TEM was employed to higher yielded elution fraction of AgNP, i.e. elution fraction 9 (Figure 6c), and the average diameter of spherical AgNP was 17 ±5 nm. From the TEM micrographs, it is evident that AgNP were uniformly distributed and well dispersed in the grid. The strong signal of C and Cu is attributed to the composition of TEM grid (carbon coated copper grid). Furthermore, the elemental mapping of purified AgNP was investigated through HAADF-STEM (Figure 6d).
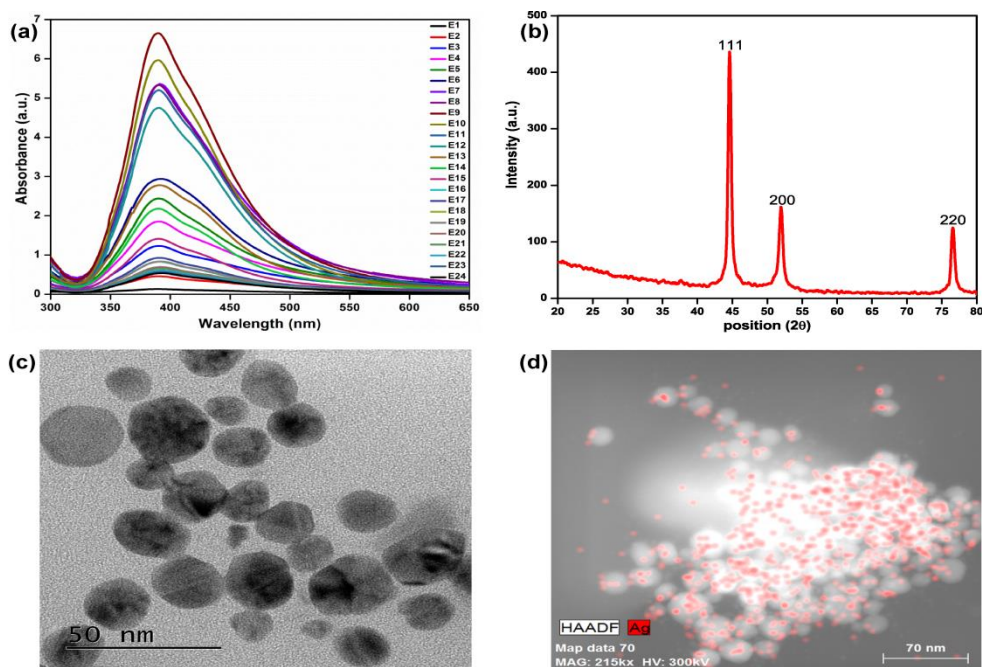
Figure 8 *Characterization of AgNP. (a) UV-Visible spectra of all fractions of AgNPs after SEC purification, (b) XRD spectrum, (c) TEM image of AgNP dispersed over carbon coated copper grid, (d) HAADF elemental mapping of AgNP in STEM mode.*

The red color patches in HAADF image represents the amount of elemental silver in AgNP, thus confirming the nanometer size particle visible at TEM grids are made of silver element. Again, the elemental composition of AgNP was examined through EDX spectroscopy present with TEM (Figure 7a). EDX spectrum shows the signal of Ag in addition to C and Cu signals. The hydrodynamic size and surface potential of AgNP analyzed using Zetasizer was 25.44 nm and -28.1 mV, respectively (Figure 7b and 7c). The hydrodynamic size is closely placed to the size calculated using Scherrer's equation and TEM micrographs. The high negative surface potential of AgNP confirms the stability of nanoparticles as well as the role of citrate as stabilizer/capping agent. Interestingly, the TEM results of AgNP are in good agreement of our hydrodynamic size obtained from Zetasizer, which is rarely seen; generally hydrodynamic size of particle are significantly larger than the size observed in TEM[25].
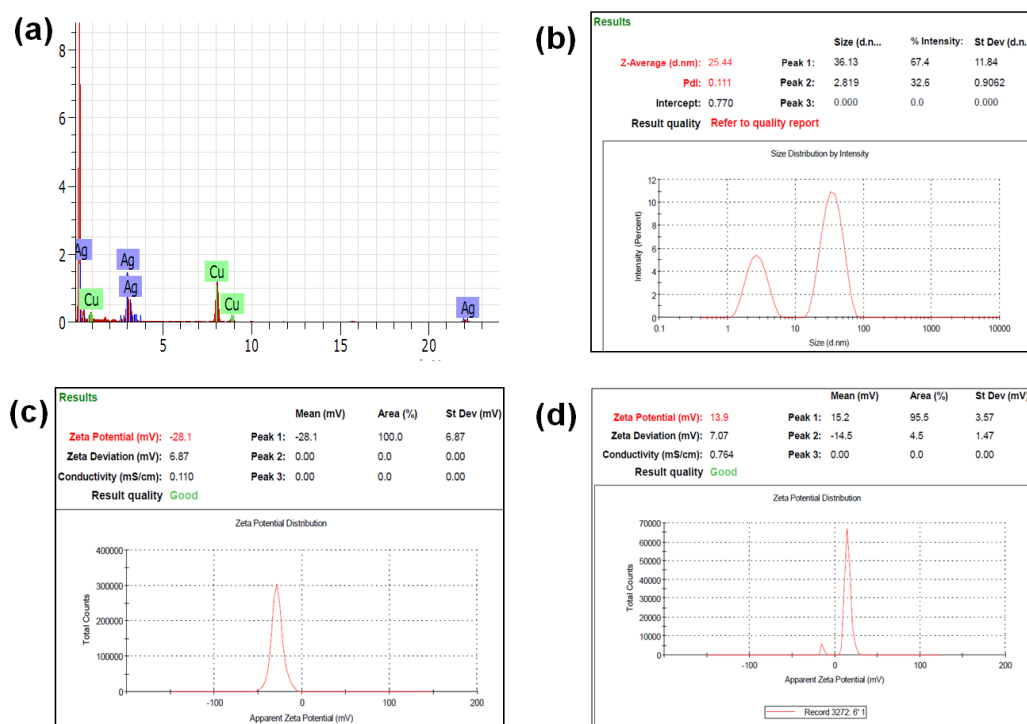
Figure 9 *(a) EDX analysis of AgNP by TEM, (b) Hydrodynamic size of AgNP, and surface potential of (c) AgNP and (d) BLf.*

2. Physico-chemical characterization of BLf-AgNP conjugates

There is an essential requirement to understand the interaction between nanoparticle and protein interface to quantify the nanoparticle properties affecting protein structure and function. When nanoparticles encounter protein in respective media, two kinetic processes compete at the same time: a) the aggregation of nanoparticles influenced by the ionic strength of media in which nanoparticles were dispersed, and b) the formation of protein corona as protective layer via adsorption to stabilize the nanoparticles against aggregation (Fig. 8a)[26]. In the aqueous solvent, AgNP is coated by BLf via physical adsorption dominated by electrostatic interaction forming primary corona followed by the secondary corona. The nanoparticles protein conjugation was initially monitored through the SPR peak of AgNP by UV-Visible spectroscopy. The SPR peak of AgNP shifted from 390 nm to 402 - 406 nm in presence of increasing BLf concentrations in solution (Fig. 8b). The red shift in the resonance band of AgNP indicated the adsorption of BLf at the nanoparticle interface, resulting into change in the local refractive index[27]. Owing to the bathochromic shift in AgNP spectra, the hydrodynamic size of AgNP after conjugation was studied using Zeta sizer[28]. On increasing concentration of BLf (1 μM to 10 μM), the average

13

hydrodynamic size of AgNP increased from 25.44 ±2.5 nm to 32.63 ±1.72 nm (Fig. 8c). Thus, increasing diameter of nanoparticle corresponds to the formation of dense protein layer at the interface[26]. Further addition of BLf (≥10 μM) signifies the total saturation of AgNP surface, as also confirmed by the maximum peak change of the particle-specific SPR. As shown in Fig. 8c, the surface potential of AgNP neutralized on increasing BLf interface from -28.1 ±6.8 mV to -5.76 ±2.8mV, in deionized water medium with pH 7.0, conductivity 0.02 mS/m and TDS 0.01 ppt. The neutralization of surface potential of AgNP by BLf (with interfacial potential +13.9 mV) suggested the presence of electrostatic interaction as a dominating force for multilayered adsorption of the protein onto nanoparticle interface (Fig. 8a). These changes in size and surface potential of nanoparticle strongly indicated the corona formation[29]. Interestingly, as also reported in previous studies, the decrease in zeta potential of nanoparticle upon interaction with the protein surface is predominantly attributed to the ionic interactions involving positively charged amino acid residues like Lys, Arg and His[29, 30]. Nevertheless, additional interactions other than electrostatic might also be involved in nanoparticle-protein complex formation. The role of electrostatic interaction on corona formation and protein stability were also reported with ubiquitin and fibrinogen proteins adsorbed onto gold nanoparticle with heterogeneous functionalities at pH 4 and 7.4 buffers, below and above the isoelectric point of the protein[31]. Additionally, few surface functionalities reported to have deteriorated effects on protein and nanoparticle; protein were shown to aggregate at the interface on interaction, whereas nanoparticle loses its dispersity and dissolution changes[31, 32]. In contrast, the BLf corona established a steric repulsion barrier, which prevented the metal surface to come in contact with other metal surface, otherwise leading into agglomeration[30, 33].

(a) Charge Neutralization   Primary Corona formation   Secondary Corona formation
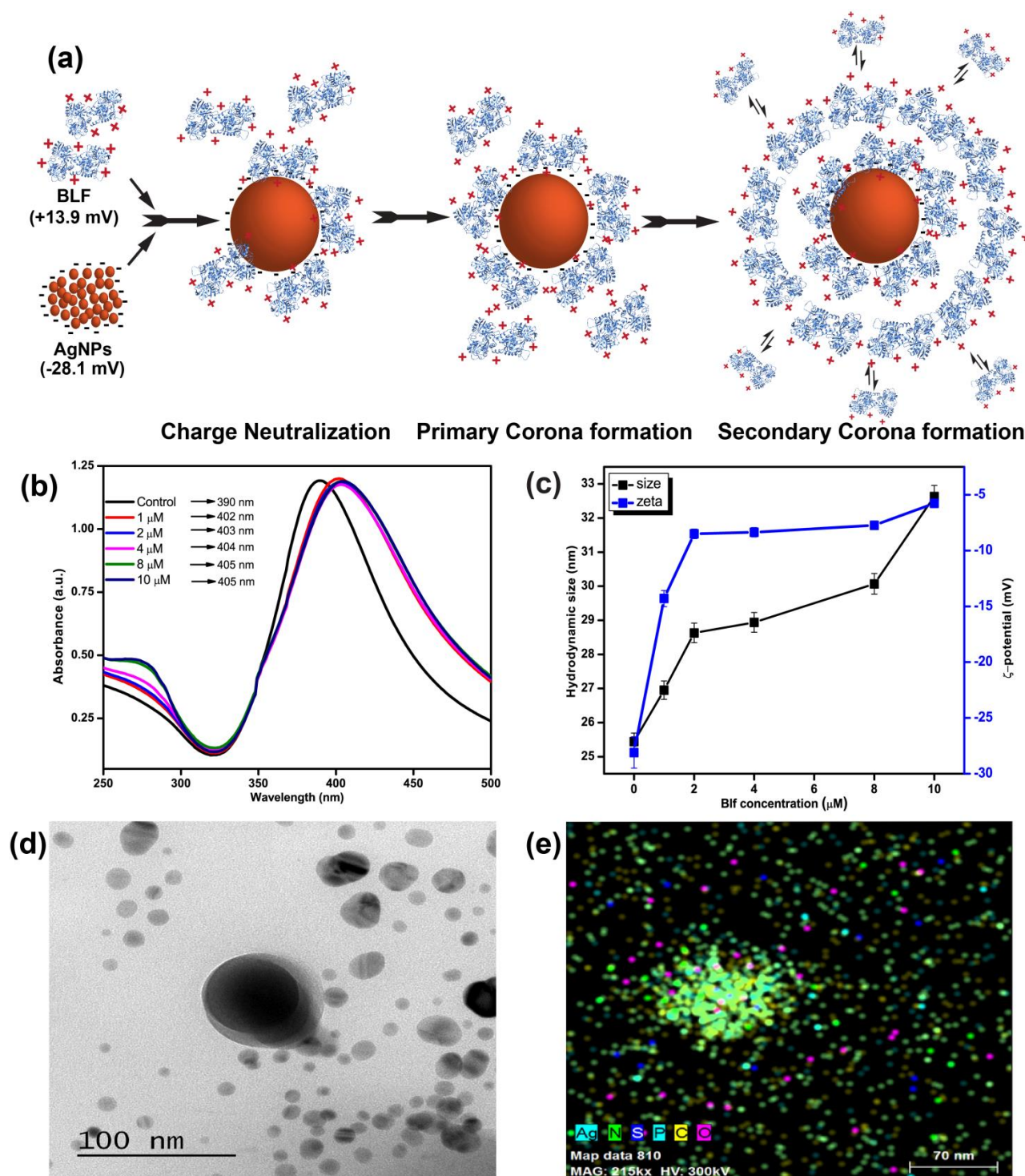
Figure 10. Characterization of BLf-AgNP conjugates. (a) Illustration of BLf adsorption onto AgNP and its surface neutralization. (b) UV-Visible spectra of AgNP in absence (control) and presence of varying concentrations of BLf (1 - 10 μM), and the wavelength indicated by the arrow mark is peak maxima in presence of respective protein concentration in BLf-AgNP conjugate. (c) Surface potential neutralization and hydrodynamic size analysis of AgNP in presence of different

15

concentration of BLf (0 - 10 μM). (d) TEM analysis of BLf-AgNP conjugates dispersed over carbon coated grid, and (e) HAADF-STEM elemental mapping of the conjugate.

The surface morphology, particle size and distribution were characterized by TEM. The BLf conjugated AgNP were predominantly spherical in shape with size 20 ±10 nm (Figure 8d). TEM micrographs revealed very little difference in size of BLf-AgNP and AgNP only, although the standard deviation is higher which can be attributed to heterogeneous adsorption of BLf on the interface; hydrodynamics size varies predominantly with change in number of protein in corona (Figure 8c). For approximate quantification of BLf in corona, largest size BLf-AgNP conjugate in TEM micrographs was considered, as shown in Figure 9. Figure 9 indicated a diffused layer of BLf corona surrounding the large sized AgNP in BLf-AgNP complex, but was absent in AgNP only samples (Figure 6c). This spherical layer has previously been reported as "core-shell structure" around the nanoparticle[34]. The width of the protein layer varied from ~1 nm to 10 nm, which has previously been divided into soft corona that readily exchanges with non-adsorbed protein and a hard corona that has higher affinity with particle core[35, 36]. Assuming BLf as a sphere with approximately 5 nm diameter[37], the calculation of diffused layer around the interface, using image J[38], suggested that about 40 to 1650 BLf molecules are adsorbed onto AgNP interface in a multilayer fashion (Figure 9). To check the elemental composition of BLf-AgNP conjugate, HAADF elemental mapping was performed in STEM mode (Figure 8e). Unlike intact AgNP (Figure 6d), the HAADF-STEM mapping of BLf-AgNP solution revealed the presence of N, O, S, C and P in addition to Ag (Figure 8e). Presence of N, O and S confirmed the organic layer to be protein (BLf) around AgNP; P is coming from the phosphate buffer, whereas C is contributing from grid composition as well as from protein. Thus, the data, altogether, indicated that the BLf conjugated to AgNP and, as the BLf fraction was increased in conjugation mixture, the size, surface potential and SPR property of the particle significantly changed.
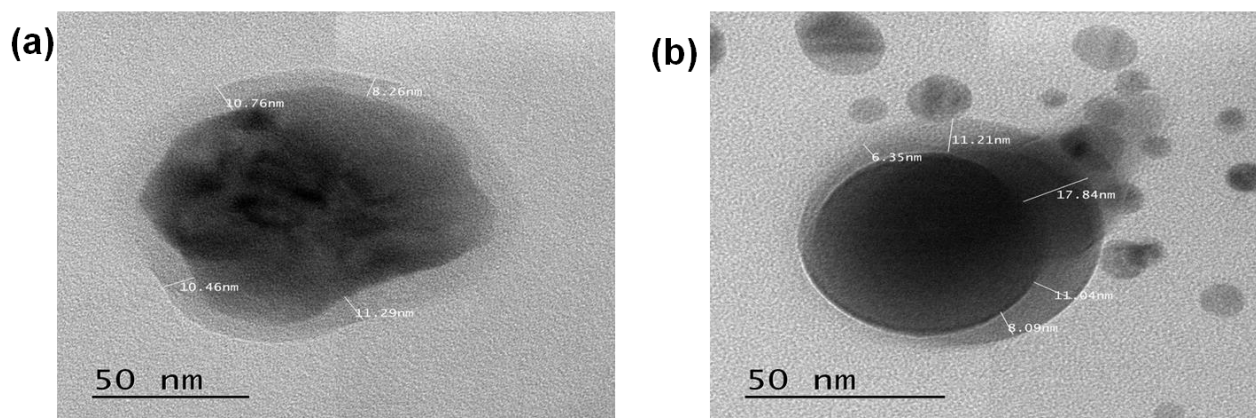
Length of scale=50 nm = 732 pixel
Length of NPs with corona (fig. 3Sb)=1120 = 76.5 nm
Length of only NPs= 832 = 56.8 nm
a. Area of complete sphere= $4/3pr^2$ = $4/3*3.14* 72.75^2$ = 18385 nm^2
b. Area of only nanoparticle= $4/3pr^2$ = $4/3*3.14* 62.5^2$ = 10135 nm^2
Avg. no. of BLf molecules over NPs surface=a-b/5 = 8250/5= 1650
But for small size AgNP, the number of molecules varies from 40 to 1209[37]

Figure 11 *Quantification of average number of BLf molecules adsorbed over AgNP interface from TEM image.*

3. FTIR and CD spectroscopy

To determine changes in secondary structure of protein on conjugation with the nanoparticle, we analyzed the FTIR spectra for BLf in absence and presence of AgNP (Figure 12a). Figure 12a indicates two dominating bands at ~1550 and 1650 cm^{-1} confirming the characteristic protein amide-II and amide-I bonds vibration peak, respectively. However, the change in amide-I and amide-II bonds in the raw spectra is found to be insignificant for BLf in presence of AgNP. Therefore, the change in secondary structure was then studied through the second derivative of amide-I bond spectra in the range of 1600-1700 cm^{-1} (Figure 12b). Dong A. *et al.* reported the distribution of secondary structure in amide-I component of a globular protein is exactly identical to the amount computed from crystallographic data[39]. As shown in Figure 12b, the second derivative of amide-I component showed that all the typical secondary structure like α-helix, β-sheet and β-turns are present in BLf. The bands at 1625 and 1637 cm^{-1} are often associated with β-sheet. The band at 1650 cm^{-1} is associated with α-helix, and the bands at 1675 and 1682 cm^{-1} are associated with β-turns. The significant increase in peak intensity was observed than for the protein in absence of the nanoparticle, which is possibly because of enhanced local BLf concentration at

17

the interface. Although, increase in interface concentration showed insignificant change in intensity and peak maxima.
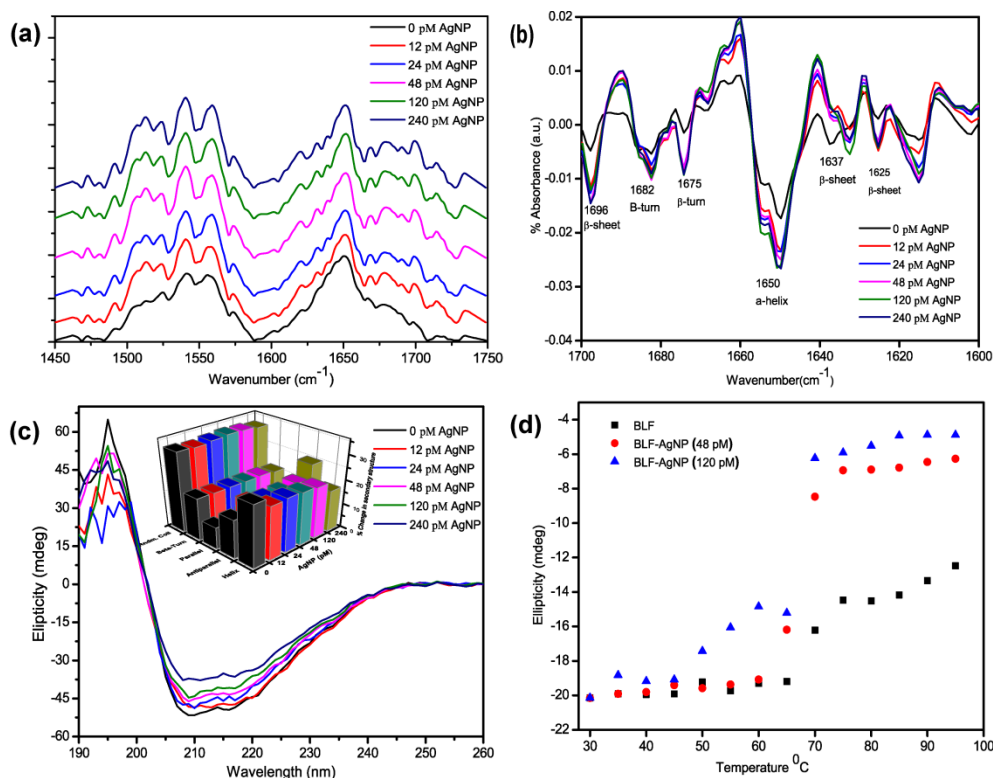
Figure 12. Secondary structure analysis of BLf in presence of different concentrations of AgNP (0 -250 pM). (a) and (b) FT-IR spectra of BLf and its 2nd derivative of amide-I stretch to resolute the secondary structure in presence of different concentrations of AgNP. (c) Change in CD spectra of BLf in presence of different AgNP concentrations, and (d) T_m of BLf in absence and presence of 48 and 120 pM AgNP concentrations.

Furthermore, the conformation of BLf was analyzed by CD spectroscopy. CD spectroscopy is an important technique to determine the change in secondary structure of protein, like α-helices, β-sheet and random coil[40]. The CD spectra of BLf in presence of varying concentrations of AgNP were shown in Figure 12c. As shown in Figure 12c, BLf exhibited two negative bands at 208 and 218 nm in the UV region, the characteristic spectra of an α/β protein[41]. Ellipticity for both the negative peaks, at 208 nm and 218 nm, decreased with increase in AgNP concentration in solution. However, the change in α-helical and β-sheet content in protein was insignificant at lower concentration, indicating the adsorption onto interface contributes insignificantly in the protein ellipticity change. On the other hand at higher concentration (240 pM AgNP), a significant change

18

in secondary structure fractions were observed; the relative percentage of α-helix content in BLf decreased from 25.21% to 16.99% while anti-parallel β-sheet showed a relative increase from 15.74% to 24.87% (Figure 12c inset). Nevertheless, no significant changes were observed in β-turn and random coil fraction for studied AgNP concentrations. Although some loss of α-helix occurred, BLf retained more than 65% of its secondary structure on interaction with AgNP, even to highest AgNP concentration (240 pM). The observation indicated that the local conformational changes, irrespective of global protein structure, happened on binding to NP surface. The increased β-sheet content at highest studied AgNP concentration indicated fraction of the α-helix conformation is undergoing conformational change into anti-parallel β-sheet during the protein-nanoparticle interaction and corona stabilization. This suggests that BLf conformation changes when exposed to highest AgNP concentration, but remains stabilized at lower concentration.

CD spectra were also used to analyze the temperature-mediated stability of BLf in presence of AgNP. The spectra of BLf for 190-260 nm were collected in the temperature range of 25-90 ^{o}C with a step of 5 ^{o}C. The thermal unfolding of BLf was also studied in presence of 48 pM and 120 pM AgNP, and compared to BLf only thermogram. Figure 12d showed the decrease in negative ellipticity plotted at 280 nm of BLf with rise in temperature and fitted to a Boltzmann equation,

$$y = A+ (B-A)/(1+\exp(x-x_o)/dx)$$

Where x is the temperature, x_o is the melting temperature (T_m), and dx the width of the thermal transition, A and B are constant, using a non-linear square fitting algorithm present in Origin software (OriginLab 7.0). The thermal unfolding of BLf in absence of AgNP has shown a steep unfolding transition with a (T_m) of 69.9 ±1.1 ^{o}C with a width of 3.86 ±0.97 inferring a cooperative thermal protein unfolding reaction. On the other hand, the Tm of BLf-AgNP conjugate decreased to 66.75 ±0.21 and 65.67 ±1.43 ^{o}C (in presence of 48 pM AgNP and 120 pM AgNP, respectively). Although the T_m of BLf decreased with increase in AgNP concentration, but temperature-mediated unfolding of BLf in presence of AgNP remained a cooperative unfolding process, inferring overall protein structure remains significantly comparable to the intact protein.

4. Antimicrobial propensity of the BLf-AgNP conjugates

Previous studies have suggested that hololactoferrin has ferric ions, which is sequestered by bacteria in their metabolic processes. We therefore, used iron deficient lactoferrin (a.k.a. apolactoferrin) for antibacterial assay through arresting their growth kinetics, i.e. acting as a

bacteriostatic agent. In order to investigate the antibacterial activity of BLf-AgNP conjugates, IC_{50} value of BLf and AgNP was observed separately against *E. coli* and *S. aureus* (Fig. 13a and 13b). The figures indicated that presence of increasing concentration of AgNP and BLf significantly inhibited the bacterial growth. The IC_{50} value of BLf and AgNP was 312 µg/mL (4 µM) and 20 µg/mL (48 pM) respectively, for both *E. coli* and *S. aureus*. Hence, to examine the effect of BLf-AgNP conjugate on bacteria, the optimized IC_{50} concentration of BLf and AgNP were taken for conjugation prior to observe antimicrobial effect of the conjugate on bacterial growth kinetics (Fig. 13c). Growth kinetic results showed that the bacteriostatic property of BLf remains unaltered in the conjugate, but the extent of antimicrobial activity may vary depending upon the local concentration of AgNP. Interestingly the amino acid at the iron binding sites in N-lobe (Asp60, His253, Tyr92) and C-lobe (Arg121, Tyr192) are not listed in the close proximity of AgNP interface (Table 1), further suggested that AgNP binding will not affect the bacteriostatic activity of BLf. The stable BLf-AgNP interface also rationalized their non-synergistic antimicrobial effect against bacteria.
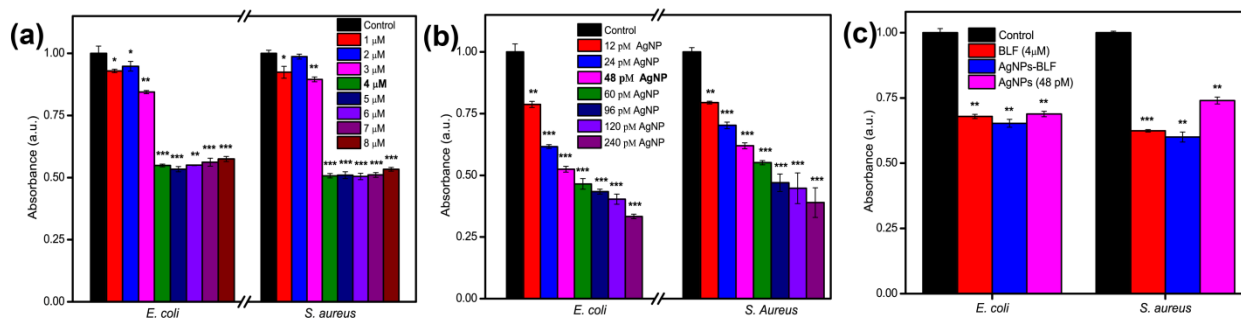
Figure 13. Antimicrobial activity of BLf-AgNP conjugates. Growth of *E. coli* and *S. aureus* in presence of different concentrations of BLf only (a), AgNP only (b) and BLf-AgNP conjugate (c). The error bar indicates ±S.E.M. of three independent experiments with respective significance value, *: $P < 0.05$; **: $P < 0.01$; ***: $P < 0.001$, compared to control.

Table 1. Table enlists the residues that are found at the protein-NP interfaces and the shifts during simulations for both the N- and C- lobes (as obtained from simulation study performed at Tezpur University).

N-Lobe	C-Lobe
172L	620K
173C	621N
174K	622G

20

175G	623K
176E	624N
177G	625P
180N	626P
181C	633K
182A	415R
183C	416K
184S	417S
185S	418S
186R	421S
187E	422S
188P	553N
189Y	554S

5. Isolation, purification and antimicrobial efficacy of AMP from Lactic acid bacteria

Lactic acid bacteria (LAB) are well known to suppress food spoilage and growth of pathogenic bacteria by producing array of antimicrobial compounds including small proteins and peptides known as bacteriocins[31, 32]. Among all, lacticin 3147 is a broad-spectrum bacteriocin produced by *Lactococcus lactis* subsp. *lactis* DPC3147 [33]. Work done by M. P. Ryan and group suggest that lacticin 3147 acts on a broad range of gram-positive bacteria via pore formation [34]. We tried to isolate lacticin following the procedure developed by Lasta S *et al*., 2012 with certain modifications. Briefly, the lacticin producing strain *Lactococcus lactis* subspecies *lactis* was allowed grow till early stationary-phase in M17 medium. After incubation the culture was subjected to centrifugation (10,000 rpm, 4 °C for 10 min) to remove cells and obtained supernatant was then filtered using 0.45 μm pore sized filter. The filtered supernatant was heated at 100 °C for 10 min to prevent bacteriocin proteolysis and subjected to 60 % ammonium sulphate precipitation. The resulting suspension was centrifuged at 10,000 rpm 40 min and the obtained pellet was re-dissolved in 50 mM sodium phosphate buffer pH 6.8 and dialysed three times against double-distilled water for 24 h. The dialysed crude extraxt was fractioned using 10 kD Centricon (Amicon ultra-15 centrifugal filter unit, merkmillipore, Germany) at 4000rpm for 20 min. The dialysed fraction was run on SDS PAGE to check the presence of lacticin in the crude extract. Figure 14a shows silver stained gel with a light band developed near ~3kD region corresponding to lacticin. Furthermore, the conformation of crude AMP extract was analysed by CD spectroscopy. As shown in Figure

14b, crude AMP extract exhibited two negative bands at 208 and 218 nm in the UV region, the characteristic spectra of an α/β protein[41]. The antimicrobial assay was performed with different concentration of retentate and permeate obtained after centicon against Gram-positive *B. subtilis* and Gram-negative *E* (Figure 15 a-d)*. coli*. Both factions showed comparable inhibition against both stains which suggest that apart from lacticin some other agents present in the crude extract is responsible for inhibition. To get a clear picture we need to proceed with further purification protocol, but unfortunately the inaccessibility of the funds has restrained us to do so and carry-on other related experimentations.
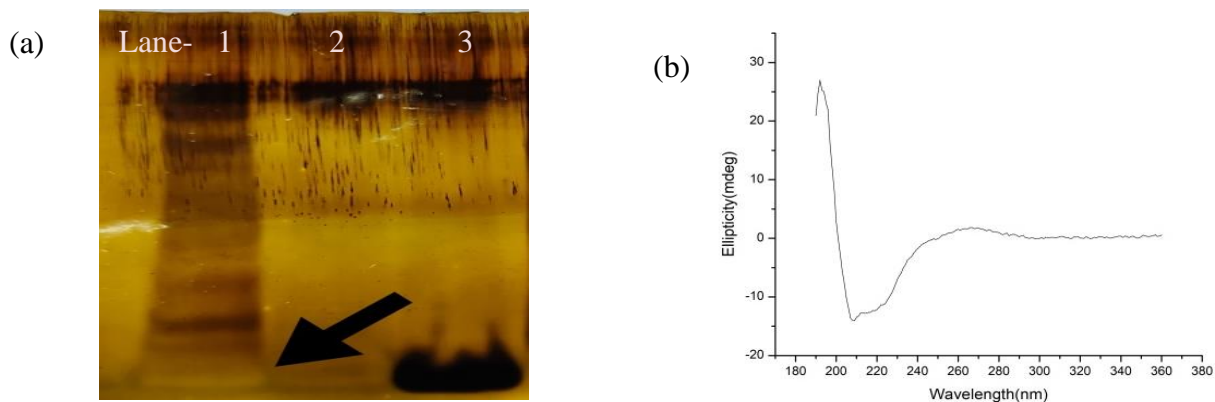
Figure 14. Crude AMP extract a) Silver stained SDS-Polyacrylamide gel lane 1- crude extract, 2-Nil,3-Insulin (marker) ; b) CD spectra
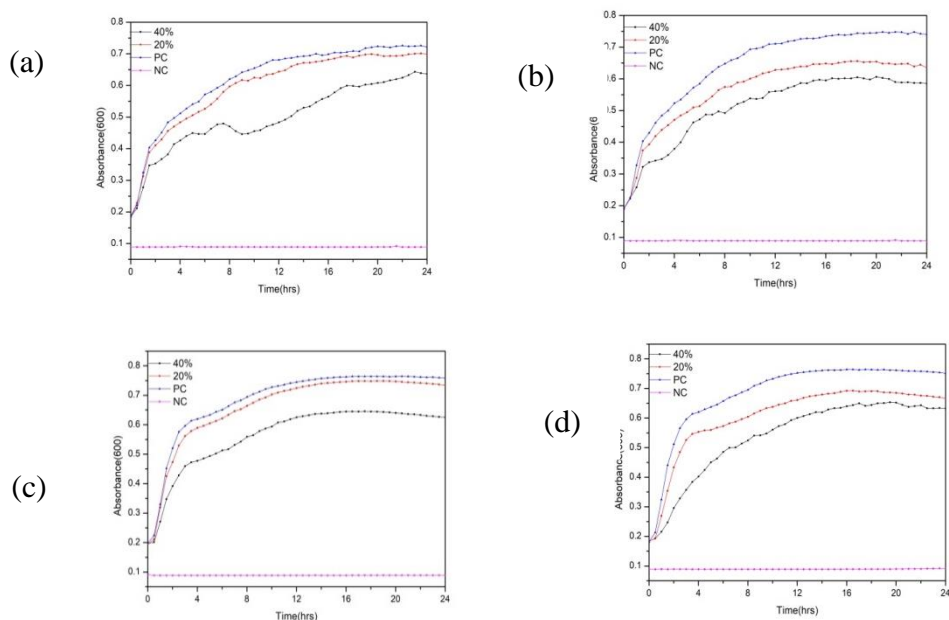
Figure 15. Antimicrobial activity of AMP crude extract obtained from *Lactococcus lactis* subsp. *lactis*. Growth of *B. subtilis* and *E. coli* in presence of different concentrations of permeate- BS (a),retentate- BS (b) and permeate- EC (c),and retentate-EC (d) with respect to control.

References

1.   Zasloff, M., *Antimicrobial peptides of multicellular organisms.* Nature, 2002. **415**: p. 389.

2.   Alves, C.S., et al., *Escherichia coli cell surface perturbation and disruption induced by antimicrobial peptides BP100 and pepR.* Journal of Biological Chemistry, 2010. **285**(36): p. 27536-27544.

3.   Li, X., et al., *Functional gold nanoparticles as potent antimicrobial agents against multi-drug-resistant bacteria.* ACS nano, 2014. **8**(10): p. 10682-10686.

4.   Tiwari, P.M., et al., *Functionalized gold nanoparticles and their biomedical applications.* Nanomaterials, 2011. **1**(1): p. 31-63.

5.   Nel, A.E., et al., *Understanding biophysicochemical interactions at the nano–bio interface.* Nature materials, 2009. **8**(7): p. 543-557.

6.   Panáček, A., et al., *Silver colloid nanoparticles: synthesis, characterization, and their antibacterial activity.* J. Phys. Chem. B, 2006. **110**(33): p. 16248-16253.

7.   Gordon, Y.J., E.G. Romanowski, and A.M. McDermott, *A review of antimicrobial peptides and their therapeutic potential as anti-infective drugs.* Curr Eye Res, 2005. **30**(7): p. 505-15.

8.   Peschel, A. and H.G. Sahl, *The co-evolution of host cationic antimicrobial peptides and microbial resistance.* Nat Rev Microbiol, 2006. **4**(7): p. 529-36.

9.   Peschel, A. and H.-G.J.N.R.M. Sahl, *The co-evolution of host cationic antimicrobial peptides and microbial resistance.* 2006. **4**(7): p. 529.

10.   Hancock, R.E. and G.J.T.i.m. Diamond, *The role of cationic antimicrobial peptides in innate host defences.* 2000. **8**(9): p. 402-410.

11.   Brogden, K.A.J.N.r.m., *Antimicrobial peptides: pore formers or metabolic inhibitors in bacteria?* 2005. **3**(3): p. 238.

12.   Alves, C.S., et al., *Escherichia coli cell surface perturbation and disruption induced by antimicrobial peptides, BP100 and pepR.* 2010: p. jbc. M110. 130955.

13.   Hasper, H.E., B. de Kruijff, and E. Breukink, *Assembly and stability of nisin− lipid II pores.*

23

Biochemistry, 2004. **43**(36): p. 11567-11575.

14. Korbekandi, H. and S. Iravani, *Silver nanoparticles*, in *The delivery of nanoparticles*. 2012, InTech.

15. Van Der Spoel, D., et al., *GROMACS: fast, flexible, and free.* Journal of computational chemistry, 2005. **26**(16): p. 1701-1718.

16. Baker, E.N., *Structure and Reactivity of Transferrins*, in *Advances in Inorganic Chemistry*, A.G. Sykes, Editor. 1994, Academic Press. p. 389-463.

17. Moore, S.A., et al., *Three-dimensional structure of diferric bovine lactoferrin at 2.8 Å resolution11Edited by D. Rees.* Journal of Molecular Biology, 1997. **274**(2): p. 222-236.

18. Bader, M.W., et al., *Recognition of antimicrobial peptides by a bacterial sensor kinase.* 2005. **122**(3): p. 461-472.

19. Lominadze, G., et al., *Proteomic analysis of human neutrophil granules.* 2005. **4**(10): p. 1503-1521.

20. Berman, H.M., et al., *The protein data bank.* 2000. **28**(1): p. 235-242.

21. Tan, K.W., et al., *Structural basis for the bacterial membrane insertion of dermcidin peptide, DCD-1L.* 2017. **7**(1): p. 13923.

22. Murzyn, K., T. Róg, and M.J.B.j. Pasenkiewicz-Gierula, *Phosphatidylethanolamine-phosphatidylglycerol bilayer as a model of the inner bacterial membrane.* 2005. **88**(2): p. 1091-1103.

23. Knight, C.J. and J.S.J.B. Hub, *MemGen: A general web server for the setup of lipid membrane simulation systems.* 2015. **31**(17): p. 2897-2899.

24. Van Der Spoel, D., et al., *GROMACS: fast, flexible, and free.* 2005. **26**(16): p. 1701-1718.

25. Nayak, P.S., et al., *An approach towards continuous production of silver nanoparticles using Bacillus thuringiensis.* RSC Advances, 2016. **6**(10): p. 8232-8242.

26. Piella, J., N.G. Bastús, and V. Puntes, *Size-dependent protein–nanoparticle interactions in citrate-stabilized gold nanoparticles: the emergence of the protein corona.* Bioconjugate chemistry, 2016. **28**(1): p. 88-97.

27. Yang, J.A., et al., *Study of wild-type α-synuclein binding and orientation on gold nanoparticles.* Langmuir, 2013. **29**(14): p. 4603-4615.

28. Gagner, J.E., et al., *Effect of gold nanoparticle morphology on adsorbed protein structure and function.* Biomaterials, 2011. **32**(29): p. 7241-7252.

29. Casals, E., et al., *Time evolution of the nanoparticle protein corona.* ACS nano, 2010. **4**(7):

p. 3623-3632.

30. Goy-López, S., et al., *Physicochemical characteristics of protein–NP bioconjugates: the role of particle curvature and solution conditions on human serum albumin conformation and fibrillogenesis inhibition.* Langmuir, 2012. **28**(24): p. 9113-9126.

31. Huang, R., et al., *Protein–nanoparticle interactions: the effects of surface compositional and structural heterogeneity are scale dependent.* Nanoscale, 2013. **5**(15): p. 6928-6935.

32. Tejamaya, M., et al., *Stability of citrate, PVP, and PEG coated silver nanoparticles in ecotoxicology media.* Environ. Sci. Technol, 2012. **46**(13): p. 7011-7017.

33. Landgraf, L., et al., *A plasma protein corona enhances the biocompatibility of Au@ Fe 3 O 4 Janus particles.* Biomaterials, 2015. **68**: p. 77-88.

34. Winuprasith, T., et al., *Alterations in nanoparticle protein corona by biological surfactants: Impact of bile salts on β-lactoglobulin-coated gold nanoparticles.* Journal of colloid and interface science, 2014. **426**: p. 333-340.

35. Rahman, M., et al., *Nanoparticle and protein corona*, in *Protein-nanoparticle interactions*. 2013, Springer. p. 21-44.

36. Cedervall, T., et al., *Understanding the nanoparticle–protein corona using methods to quantify exchange rates and affinities of proteins for nanoparticles.* Proceedings of the National Academy of Sciences, 2007. **104**(7): p. 2050-2055.

37. Erickson, H.P., *Size and shape of protein molecules at the nanometer level determined by sedimentation, gel filtration, and electron microscopy.* Biological procedures online, 2009. **11**(1): p. 32.

38. Ferreira, T. and W. Rasband, *ImageJ user guide.* ImageJ/Fiji, 2012. **1**.

39. Dong, A., P. Huang, and W.S. Caughey, *Protein secondary structures in water from second-derivative amide I infrared spectra.* Biochemistry, 1990. **29**(13): p. 3303-3308.

40. Whitmore, L. and B.A. Wallace, *Protein secondary structure analyses from circular dichroism spectroscopy: methods and reference databases.* Biopolymers, 2008. **89**(5): p. 392-400.

41. Rabbani, G., et al., *Effect of copper oxide nanoparticles on the conformation and activity of β-galactosidase.* Colloids and Surfaces B: Biointerfaces, 2014. **123**: p. 96-105.

FINALCONSOLIDATED STATEMENT OF EXPENDITURE
(FOR FINAL SETTLEMENT OF ACCOUNTS)

1. Title of the Project   : Nanoparticle based approach to enhance the AMP efficacy against AMP resistant bacteria
2. Sanctioned Project Cost   : 29.29 Lakhs
3. Revised cost, if any   : NA
4. Duration of the project   : 3.5 years
5. Sanction Order No. & Date   : BT/PR15941/NER/95/33/2015
6. Date of commencement of Project   : 18 Oct 2016
7. Extension, if any   : 06 months
8. Date of completion of project   : 17 Apr 2020

Details of grant, expenditure and balance

S.No.	Heads	Sanctioned Cost	Year-wise Releases made					Year-wise Expenditure incurred						Balance
			1st yr.	2nd yr.	3rd yr.	4th yr.	Total	1st yr.	2nd yr.	3rd yr.	4th yr.	5th yr.	Total	
			18 Oct 2016- 31 Mar 2017	01 Apr 2017- 31 Mar 2018	01 Apr 2018 - 31 Mar 2019	01 Apr 2019- 31 Mar 2020		18 Oct 2016- 31 Mar 2017	01 Apr 2017- 31 Mar 2018	01 Apr 2018 - 31 Mar 2019	01 Apr 2019- 31 Mar 2020	01 Apr 2020- 17 Apr 2020		
	A. Non-recurring page no.-													
	Equipment	10.0	10.00	0.00	0.00	0.00	10.00	0.00	10.00	0.00	0.00	0.00	10.00	0.00
	B. Recurring													
1.	Manpower	10.29	3.30	0.00	2.35	1.692	7.342	0.60	2.35	2.54	1.54	0.21933	7.24933	0.09267
2.	Consumables	3.00	1.00	0.00	1.00	0.417	2.417	0.3471	0.71343	0.94462	0.41185	0.00	2.417	0.00000
3.	Travel	1.50	0.50	0.00	0.50	0.199	1.199	0.2876	0.33741	0.36554	0.49277	0.00	1.48332	-0.28432
4.	Contingency	1.50	0.50	0.00	0.43	0.208	1.138	0.43006	0.00	0.51809	0.00	0.00	0.94815	0.18985
5.	Overhead	3.00	1.00	0.00	0.43	0.154	1.584	0.62500	0.17756	0.59383	0.22639	0.17955	1.80233	-0.21833
6.	Interest earned	0.00	0.19346	0.02373	0.01191	0.00726	0.23636	0.00	0.00	0.00	0.00	0.00	0.00	0.23636
	Total	19.29	6.49346	0.02373	4.72191	2.67726	13.91636	2.28976	3.5784	4.96208	2.67101	0.39888	13.90013	0.01623
	Grand Total (A+B)	29.29	16.49346	0.02373	4.72191	2.67726	23.91636	2.28976	13.5784	4.96208	2.67101	0.39888	23.90013	0.01623

(PROJECT INVESTIGATOR)
Dr.Anupam Nath Jha
Assistant Professor
Dept of Molecular Biology & Biotechnology
Tezpur University, Tezpur - 784028

(HEAD OF THE INSTITUTE)
Registrar
Tezpur University

(FINANCE OFFICER)
Finance Office
Tezpur University

Details of Assets acquired wholly or substantially out of Govt. grants
Register to be maintained by Grantee Institution

1. Name of the Sanctioning Authority: Department of Biotechnology

2. Name of the Grantee Institution   Tezpur University

3. No. & Date of sanction order   BT/PR15941/NER/95/33/2015 dated Oct 18 2016

4. Amount of the sanctioned grant   16.30 Lakhs

5. Brief purpose of the grant   Nanoparticle based approach to enhance the AMP efficacy against AMP resistant bacteria

6. Whether any condition regarding the
    right of ownership of Govt. in the
    Property or other assets acquired
    out of the grant was incorporated
    in the grant-in-aid sanction order.   Yes

*7. Particulars of assets actually credited
    or acquired.

Sl. No.	Asset	Status	Value
1	Computer Workstations	Installed in April	10 Lakhs

8. Value of the assets as on 31/03/2020   Rs. 10.00 Lakhs

9. Purpose for which utilised at present Installation has been done to perform long timescale MD Simulation

10. Encumbered or not   No

11. Reasons, if encumbered   NA

12. Disposed of or not   NA

13. Reasons and authority, if any, for
    Disposal   NA

14. Amount realised on disposal   NIL

15. Remarks   NO

(PROJECT INVESTIGATOR)

Dr.Anupam Nath Jha
Assistant Professor
ot of Molecular Biology & Biotechnol
Tezpur University, Tezpur - 784028

(HEAD OF THE INSTITUTE)

Registrar
Tezpur University

(FINANCE OFFICER)

Finance Officer
Tezpur University

Utilisation Certificate

(for the financial year 2020-2021)

(Rs. in Lakhs)

1. Title of the Project/Scheme: **Nanoparticle based approach to enhance the AMP efficacy against AMP resistant bacteria**

2. Name of the Organisation: Tezpur University, Napam, Tezpur, Assam

3. Principal Investigator: Dr Anupam Nath Jha

4. Deptt. of Biotechnology sanction order No. & date of sanctioning the project: BT/PR15941/NER/95/33/2015 dated Oct 18 2016

5. Amount brought forward from the previous financial year quoting DBT letter No. & date in which the authority to carry forward the said amount was given: 0.41511 Lakhs

6. Amount received from DBT during the financial year (*please give No. and dates of sanction orders showing the amounts paid*): NIL

7. Other receipts/interest earned, if any, on the DBT grants: NIL

8. Total amount that was available for expenditure during the financial year (Sl. Nos. 5,6 and 7): 0.41511 Lakhs

9. Actual expenditure (excluding commitments) incurred during the financial year (statement of expenditure is enclosed): 0.39888 Lakhs

10. Unspent balance refunded, if any (Please give details of cheque No. etc.): NA

11. Balance amount available at the end of the financial year: 0.01623 Lakhs

12. Amount allowed to be carried forward to the next financial year vide letter No. & date: 0.01623 Lakhs

1. Certified that the amount of Rs. **0.39888 Lakhs** mentioned against col. 9 has been utilised on the project/scheme for the purpose for which it was sanctioned and that the balance of Rs **0.01623 Lakhs** will be returned.

2. Certified that I have satisfied myself that the conditions on which the grants-in-aid was sanctioned have been duly fulfilled/are being fulfilled and that I have exercised the following checks to see that the money was actually utilised for the purpose for which it was sanctioned.

Kinds of checks exercised:

1. Cash Book

2. Ledgers

3. Vouchers

4. Bank Statements

5. Any other

(PROJECT INVESTIGATOR)
Dr.Anupam Nath
Assistant Professor
Dept of Molecular Biology & Biotechnology
Tezpur University, Tezpur - 784028

(FINANCE OFFICER)
Finance Officer
Tezpur University

(HEAD OF THE INSTITUTE)
Registrar
Tezpur University

"Nanoparticle based approach to enhance the AMP efficacy against AMP resistant bacteria"   Annexure-II

Statement of Expenditure referred to in Para 9 of the Utilization Certificate

Showing grant received from the Department on Biotechnology and the expenditure incurred during the financial year 2020-2021

Rs. In Lakh

Items	Unspent balance carried forward from previous year	Grants received from the DBT during the year	Other receipts/interest earned if any, on the DBT grants	Total of col. (3+4+5)	Expenditure (Excluding commitments incurred during the year)	Balance (5-6)	Remarks
1	2	3	4	5	6	7	8
I. Non-Recurring							
(i) Equipments	0.00	NIL	NIL	NIL	0	0	
Sub Total (I)	0.00	NIL	NIL	NIL	0	0	
II. Recurring							
(i) Human Resource	0.312	NIL	NIL	0.312	0.21933	0.09267	
(ii) Consumables	0.00	NIL	NIL	0.00	0.00	0.00	
(iii) Travel	-0.28432	NIL	NIL	-0.28432	0.00	-0.28432	
(iv) Contingency	0.18985	NIL	NIL	0.18985	0.00	0.18985	
(v) Overhead	0.19032	NIL	NIL	0.19032	0.17955	0.01077	
(vi) Interest Earned	0.00726	NIL	NIL	0.00726	0.00	0.00726	
Sub Total (II)	0.41511	NIL	NIL	0.41511	0.39888	0.01623	
Grand Total (I+II)	0.41511	NIL	NIL	0.41511	0.39888	0.01623	

Balance amount: One thousand six hundred and twenty three only.

PROJECT INVESTIGATOR
Dr.Anupam Nath Jha
Assistant Professor
t of Molecular Biology & Biotechnolo
ur University, Tezpur - 78....

FINANCE OFFICER
Finance Officer
Tezpur University

FOR HEAD OF THE INSTITUTE
Registrar
Tezpur University

Manpower Staffing Details (In the financial year wise manner)

For the financial year 2020-2021

From 01-04-2020 to 17-04-2020

NAME OF THE PERSON	NAME OF THE POST	DATE OF JOINING	DATE OF LEAVING	TOTAL MONTHLY SALARY	TOTAL SALARY PAID DURING THE FINANCIAL YEAR	TOTAL SALARY PAID DURING PROJECT PERIOD
Zaved Hazarika	SRF	01-01-2019	14-04-2020	Rs 14,000.00	Rs 21,933.00	Rs 21,933.00

(Signature of Principal Investigator)

Dr.Anupam Nath Jha
Assistant Professor
nt of Molecular Biology & Biotechnolo
Tezpur University, Tezpur - 784028

(Signature of Accounts Officer)
Finance Officer
Tezpur University

(SIGNATURE OF HEAD OF THE INSTITUTE)
Registrar
Tezpur University

Manpower Expenditure Details (In financial year wise manner)*:

For the financial year 2020-2021

(From 01-04-2020 to 17-04-2020)

SANCTIONED POSTS	NUMBER	SCALE OF PAY	ANNUAL OUTLAY	OUTLAY FOR THE ENTIRE PERIOD	REVISED SCALE, IF ANY	REVISED ANNUAL OUTLAY	REVISED PROJECT OUTLAY	ACTUAL RELASES BY DBT	ACTUAL EXPENDITURE	BALANCE
SRF	1	Rs 14,000	0.312 Lakhs	0.312 Lakhs	---	---	---	--	0.21933 Lakhs	0.09267 Lakhs
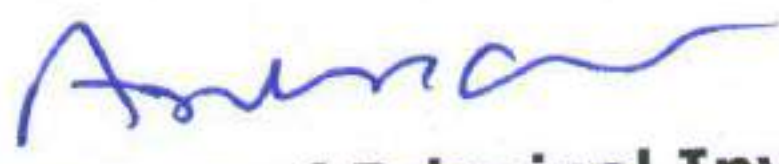
(Signature of Principal Investigator)

Jr.Anupam Nath Ji.
Assistant Professor
of Molecular Biology & Biotechno:
pur University, Tezpur - 7840?

(Signature of Accounts Officer)

Finance Officer
Tezpur University

(SIGNATURE OF HEAD OF THE INSTITUTE)
Registrar
Tezpur University

* Details of manpower salary/ fellowship revision alongwith due- drawn statement and arrears requested should be given separately, if applicable.

Due- Drawn Statement

For the financial year 2020-2021

(From 01-04-2019 to 17-04-2020)

Name of the Project Staff	Month and Year	Due	Drawn	Difference
Zaved Hazarika	NA	0.312 lakhs	0.21933 Lakhs	0.09267 Lakhs

(Signature of Principal Investigator)

Dr.Anupam Nath Jha
Assistant Professor
ot of Molecular Biology & Biotechnolo
Tezpur University, Tezpur - 784028

(Signature of Accounts Officer)

Finance Officer
Tezpur University

(SIGNATURE OF HEAD OF THE INSTITUTE)
Registrar
Tezpur University